Chemical kinetics and thermodynamics of tin ionization in H_2-O_2-N_2 flames and the proton affinity of SnO

John M. Goodings and QingFeng Chen

Abstract: A small amount ($\leq 10^{-6}$ mol fraction) of tin was introduced into five, fuel-rich, H_2-O_2-N_2 flames in the temperature range 1820–2400 K at atmospheric pressure. Ions in a flame were observed by sampling the flame along its axis through a nozzle into a mass spectrometer. The major neutral tin species in these flames were SnO (>97%) and Sn (<3%). The principal tin ions observed were $SnOH^+$ and Sn^+. Thermodynamic functions for $SnOH^+$, Sn^+, SnO, and Sn were calculated by statistical mechanics using published data from ab initio calculations and spectroscopy. The $SnOH^+$ ion was formed initially by proton transfer to SnO by H_3O^+, a natural flame ion, with which it is in equilibrium. It was also produced by chemi-ionization of SnO reacting with H; $SnOH^+$ rapidly equilibrates with Sn^+. Ion ratio measurements of $SnOH^+/H_3O^+$ led to the proton affinity PA°_{298} (SnO) = 911 ± 21 kJ mol $^{-1}$ (218 ± 5 kcal mol^{-1}). A calculated equilibrium constant provided the $SnOH^+/Sn^+$ ion ratio. When electron-ion recombination of $SnOH^+$ with free electrons was made dominant by the addition of CH_4 and K, the measured recombination coefficient of $SnOH^+$ was $(0.116 \pm 0.065)T^{-(1.66\pm0.16)}$ cm^3 molecule^{-1} s^{-1}; the temperature dependence is in good agreement with the $T^{-1.5}$ dependence predicted by simple theory. The rate constant for chemi-ionization could not be measured due to impurity ions from potassium and sodium, but the equilibrium constant for chemi-ionization/recombination was calculated to be 0.004 863 exp (–52 070/T). Assuming detailed balance and the experimental recombination coefficient, the relatively small rate constant for chemi-ionization was given by 3.27 × 10^{-10} exp (–48 630/T) cm^3 molecule^{-1} s^{-1}. Finally, calculated values were obtained for the bond energy $D^{\circ}_0(\mathrm{HO{-}Sn^+})$ = 408 ± 21 kJ mol^{-1}, and the standard zero-point enthalpy of formation $\Delta_f H^{\circ}_0(\mathrm{SnOH^+})$ = 637 ± 21 kJ mol^{-1}.

Key words: flame ionization, chemi-ionization, proton affinity, mass spectrometry, tin.

Résumé : On a introduit de faibles quantités (fraction molaire $\leq 10^{-6}$) d'étain dans cinq flammes de H_2-O_2-N_2 riches en combustible, à des températures allant de 1820 à 2400 K et à la pression ambiante. On a observé les ions dans les flammes en procédant à un échantillonnage de la flamme le long de son axe à l'aide d'une canule de spectromètre de masse. L'espèce principale d'étain dans ces flammes est le SnO (>97%) accompagnée de Sn (<3%). Les ions principaux observés sont le $SnOH^+$ et le Sn^+. Faisant appel à des méthodes de mécanique statistique et utilisant des données publiées de calculs ab initio et de spectroscopie, on a calculé les fonctions thermodynamiques du $SnOH^+$, Sn^+, SnO et Sn. L'ion $SnOH^+$ se forme initialement par un transfert de proton de H_3O^+ à SnO, un ion naturel de la flamme avec lequel il est en équilibre. Il se forme aussi par chimi-ionisation du SnO réagissant avec H; le $SnOH^+$ s'équilibre rapidement avec le Sn^+. Des mesures de rapports ioniques $SnOH^+/H_3O^+$ permettent de déterminer l'affinité protonique PA°_{298}(SnO) = 911 ± 21 kJ mol^{-1} (218 ± 5 kcal mol^{-1}). On a obtenu un rapport ionique $SnOH^+$ à l'aide de la constante d'équilibre calculée. Lorsque l'addition de CH_4 et de K fait que la recombinaison électron-ion du $SnOH^+$ avec des électrons libres devient la réaction dominante, le coefficient de recombinaison mesuré du $SnOH^+$ est égal à (0,116 ± 0,065) $T^{(-1{,}66\pm0{,}16)}$ cm^3 molécule^{-1} s^{-1}; la relation avec la température est en bon accord avec la dépendance $T^{-1{,}5}$ qui est prédite par la théorie simple. Il n'a pas été possible de mesurer la constante de vitesse de la réaction de chimi-ionisation à cause de la présence d'ions de potassium et de sodium à l'état d'impuretés; on a toutefois calculé que la constante d'équilibre chimi-ionisation/recombinaison est égale à 0,004 863 exp (–52 070/T). Si l'on fait l'hypothèse qu'il existe une balance détaillée et que l'on utilise le coefficient de recombinaison expérimental, on peut établir que la relativement faible constante de vitesse de la réaction de chimi-ionisation est donnée par l'équation 3,27 × 10^{-10} exp (–48 630/T) T cm^3 molécule^{-1} s^{-1}. Finalement, on a obtenu des valeurs calculées pour l'énergie de liaison, $D^{\circ}_0(\mathrm{HO{-}Sn^+})$ = 408 ± 21 kJ mol^{-1}, et l'enthalpie de formation au point zéro standard, $\Delta_f H^{\circ}_0(\mathrm{SnOH^+})$ = 637 ± 21 kJ mol^{-1}.

Mots clés : ionisation de flamme, chimi-ionisation, affinité protonique, spectrométrie de masse, étain.

[Traduit par la Rédaction]

Received April 2, 1998.

J.M. Goodings[1] and Q.F. Chen. Department of Chemistry, York University, 4700 Keele Street, Toronto, ON M3J 1P3, Canada.

[1] Author to whom correspondence may be addressed. Telephone: (416) 736–2100, ext. 33852. Fax: (416) 736–5936. E-mail: goodings@turing.sci.yorku.ca

Can. J. Chem. **76**: 1437–1446 (1998)

© 1998 NRC Canada

Table 1. Properties of the hydrogen–oxygen–nitrogen flames.

	Flame number				
Property	2	25	3	4	5
Equivalence ratio ϕ	1.5	1.5	1.5	1.5	1.5
$H_2/O_2/N_2$	2.74/1/2.95	3.0/1/3.5	3.18/1/4.07	3.09/1/4.74	3.12/1/5.77
Total unburnt gas flow ($cm^3\ s^{-1}$)	300	250	250	200	150
Measured flame temperature (K)	2400	2230	2080	1980	1820
Rise velocity in burnt gas ($m\ s^{-1}$)	19.8	18.6	15.6	11.4	8.4
Equilibrium burnt gas composition (mol fractions)					
H_2O	0.3460	0.3063	0.2754	0.2553	0.2249
H_2	0.1286	0.1527	0.1622	0.1390	0.1259
O_2	0.000 105 7	0.000 007 90	0.000 000 72	0.000 000 18	0.000 000 01
H	0.006 019	0.002 650	0.001 077	0.000 500 8	0.000 141 5
OH	0.003 084	0.000 795 1	0.000 213 0	0.000 088 90	0.000 017 54
O	0.000 094 69	0.000 009 35	0.000 000 99	0.000 000 23	0.000 000 01
N_2	0.5157	0.5375	0.5610	0.6052	0.6490
Percentage SnO/Sn (%)	97.1/2.9	96.9/3.1	97.0/3.0	97.6/2.4	98.1/1.9

1. Introduction

In a short note in 1969, Jensen (1) reported on the formation of tin ions when 10^{-3}–10^{-4} mol fraction of $Sn(CH_3)_4$, a rather high concentration, was introduced into a pair of H_2-O_2-N_2 flames at 2020 and 2475 K and atmospheric pressure. Using a microwave cavity resonator to measure the free electron concentration [e^-] and a mass spectrometer to sample the ions, he first showed that the $SnOH^+$ and Sn^+ ions observed were linked by a balanced (equilibrated) reaction. Further experiments indicated that the rather strongly endothermic chemi-ionization reaction of SnO with H to form $SnOH^+$ was not equilibrated in these flames. Aided by statistical thermodynamic calculations, values were obtained for the zero-point standard energy change $\Delta E_0^\circ (= \Delta H_0^\circ)$ for both reactions and the standard internal energy of formation $\Delta_f E_0^\circ(SnOH^+)$.

Very recently, Hopkinson and co-workers (2) carried out ab initio calculations of the group 14 monoxides for C, Si, Ge, and Sn to obtain their proton affinities. For tin, these were conducted at the B3LYP level of theory with wave functions optimised using density functional theory. In particular, two calculations designated A (B3LYP/DZVP) and B (B3YP/Sadlej) each provided a set of rotational and vibrational temperatures for $SnOH^+$ for statistical thermodynamic calculations. Combined with the thermodynamic data and tables for SnO from Pedley and Marshall (3) and the spectroscopic data for Sn and Sn^+ from Moore (4), this provided us with the impetus to re-examine the ionization of tin in flames.

The objectives of this study were to measure the proton affinity PA of SnO, the electron-ion recombination coefficient for $SnOH^+$ and the rate constant for chemi-ionization of SnO reacting with H using our flame-ion mass spectrometer to sample flames in the temperature range 1820–2400 K. Experimental values for PA°(SnO) by proton transfer with H_3O^+ and the recombination coefficient were obtained. For the very fast equilibrated reaction linking $SnOH^+$ and Sn^+, ion ratio measurements were falsified by cooling of the sample in the nozzle of the mass spectrometer but the equilibrium constant was calculated by statistical methods. Direct measurements of the relatively weak chemi-ionization reaction were compromised by the presence of K^+ and Na^+ impurity ions. However, values of the rate constant were obtained by calculating the equilibrium constant for chemi-ionization/recombination and multiplying it by the experimental recombination coefficient with the assumption of detailed balance.

2. Experimental

Five premixed, laminar, H_2-O_2-N_2 flames of fuel-rich composition (equivalence ratio $\phi = 1.5$) at atmospheric pressure were employed for this work spanning a temperature range 1820–2400 K. Their properties, including the calculated compositions of the equilibrium burnt gas based on the JANAF tables (5), are given in Table 1. These flames have been used extensively by Hayhurst and Kittelson who have measured their temperatures, rise velocities and free-radical compositions (6). The concentrations of free radicals overshoot their equilibrium values in the flame reaction zone and then decay downstream towards equilibrium in the burnt gas. The actual concentration is obtained using Sugden's disequilibrium parameter γ (7), defined as the ratio of the local concentration of a radical at a given position in the flame to its final equilibrium value given in Table 1; γ can achieve large values (>100) close to the reaction zone of the cooler flames before decaying downstream in the burnt gas towards unity. For fuel-rich flames where H_2O and H_2 are major product species, $\gamma_H = \gamma_{OH} \equiv \gamma$ and $\gamma_O = \gamma^2$. Plots of γ versus axial distance z are available (6) for the five fuel-rich flames listed in Table 1; thus, the radical concentrations are known at all points in the flames. These pseudo-one-dimensional (flat) flames were stabilized on a water-cooled brass burner previously described (8), consisting basically of a circular bundle of 151 stainless-steel hypodermic needle tubes. The fuel-rich flames in plug flow were cylindrical in shape with a diameter of about 12 mm.

Tin was introduced into the flames by spraying an aqueous solution of $SnCl_4 \cdot 5H_2O$ (Aldrich, 98+%) as an aerosol derived from an atomizer described previously (9) into the nitrogen supply of the premixed flame gas. This salt contained very small amounts of potassium and sodium as impurities. Spraying a 0.1 M solution introduced 9.5×10^{-7}

© 1998 NRC Canada

mol fraction of total tin into the unburnt flame gas. A small amount of a grey solid, presumably metallic tin, condensed onto the cooled sampling nozzle and mounting plate placed in front of the flame. The usual very pale blue colour of the flames developed a slightly stronger whitish luminosity with tin present. No evidence was observed for the formation of solid particles.

The five flames described in Table 1 exhibit only a low level of natural ionization. It was sometimes advantageous to add 0.25 mol% of CH_4 to the premixed flame gas to produce a high initial concentration of H_3O^+ ions stemming from the chemi-ionization of CH + O near the flame reaction zone; these ions subsequently decay downstream by electron-ion recombination. With the simultaneous addition of tin, H_3O^+ can produce tin ions by chemical ionization (CI) processes. The addition of CH_4 was small enough, however, so that the flame composition and temperature remained essentially unchanged. In other cases, it was occasionally desirable to add a small amount of KNO_3 to the tin solution sprayed by the atomizer to produce K^+ and free electrons e^- in the flame by collisional (thermal) ionization. By this means, the electron–ion recombination rate of the tin ions could be increased; there was no evidence for any direct reaction of K^+ with the tin ions. Thus, tin ionization could be enhanced early in the flame by methane and (or) suppressed later in the flame by potassium.

The burner is mounted horizontally on a motorized carriage with calibrated drive coupled to the *X*-axis of an *XY*-recorder. The flame axis *z* is accurately aligned with the sampling nozzle of the mass spectrometer. The apparatus has been described in detail previously (8) so only a brief description will be given here. Flame gas containing ions is sampled through an orifice in the tip of a conical nozzle protruding from a water-cooled sampling plate. The nozzles were fabricated by swaging a tiny electron microscope lens of Pt/Ir alloy into the tip of a 60° stainless-steel cone; orifice diameters of 0.17 and 0.20 mm were employed. Alternatively, a 60° electroformed nickel nozzle of diameter 0.20 mm exhibited less cooling of the sample in the boundary layer and was used when it was desired to minimize the formation of ion hydrates. The ions enter a first vacuum chamber maintained at 0.04 Pa (3×10^{-4} Torr), and are focused into a beam by an electrostatic lens. The beam then passes through a 3 mm orifice in the tip of a nose-cone into a second vacuum chamber pumped to a pressure below 0.003 Pa (2×10^{-5} Torr). The ions traverse a second ion lens into a quadrupole mass filter in which they have an axial ion energy of 15 eV. They are detected by a Faraday collector connected to a vibrating-reed electrometer having a grid-leak resistance of 10^{10} ohm; the ion signal is applied to the *Y*-axis of the *XY*-recorder. Thus, ion signal magnitudes quoted in the figures below as a voltage (in mV) refer to the collected ion current passing through 10^{10} ohm. By driving the flame towards the sampling nozzle, profiles may be obtained of an individual ion signal versus distance along the flame axis *z*. The zero on the *X*-axis distance scale ($z = 0$) is defined experimentally where the pressure abruptly rises when the sampling nozzle pokes through the flame reaction zone into the cooler unburnt gas upstream. The pressure is measured with an ionization gauge mounted on the second vacuum chamber.

As an alternative to individual ions, total positive ion (TPI) profiles can be measured by switching off the dc voltages to the quadrupole rods. Still with the dc voltages switched off and the spectrometer's mass dial set to a given mass number, all of the ions above that mass number are collected; e.g., TPI_{100} designates total positive ions above 100 u which includes just the tin ions whereas TPI_{12} includes all the ions (since no measureable flame ions occur below 12 u). This technique is useful in separating total tin ions from ions of low mass number such as H_3O^+, K^+, and Na^+ if present. However, the sensitivity of the mass spectrometer is different for individual ions and TPI because the former are measured at fairly high resolution whereas total ion collection amounts to zero resolution. The former sensitivity is approximately one half of the latter. Since a flame is a quasi-neutral plasma, $[TPI_{12}]$ is equal to $[e^-]$, the concentration of free electrons. It should be pointed out that no negative tin ions were detected in the FR flames.

A second method of measuring total ion signals was employed, which has a bearing on calibration procedures. With an appropriate voltage bias on the sampling plate, the total current of positive ions passing through the orifice was collected on the ion lens and nose-cone in the first vacuum chamber; it was measured with a sensitive picoammeter. This method is appealing when absolute ion concentrations must be measured because tuning errors and mass discrimination of individual ions are avoided. The total ion current was calibrated using the known rate for electron-ion recombination of H_3O^+ with e^-. With the atomizer turned off, 0.25 mol% of CH_4 was admitted. From the slope of a second-order recombination plot together with Butler and Hayhurst's rate coefficient $k = (3.6 \pm 0.5)\ T^{-2.1\pm0.7}$ cm^3 molecule^{-1} s^{-1} (10), a calibration factor was obtained for converting ion current (μA) into ion concentration (molecule cm^{-3}). The same procedure was employed with the mass spectrometer for calibrating ion signal (mV) in terms of ion concentration (molecule cm^{-3}). The calibration was routinely done for each flame when absolute ion densities were needed.

On occasion, it was noted that the ion signal slowly and steadily decreased over a period of several minutes. The worst cases occurred for the hot flames 2 and 25 when the burner was moved in close to the sampling nozzle; in these circumstances, the nozzle can become red hot. A possible explanation involves the formation of a thin layer of dielectric oxide which coats the orifice rim and subsequently acquires a positive charge which repels incoming positive ions as they approach the nozzle. Accordingly, the calibration procedure with CH_4 addition was carried out at the beginning and end of each set of tin experiments with each flame, and the results were accepted only if the calibration factor remained constant. Calibration procedures for the atomizer delivery of tin into the flame gas have been given previously (11, 12).

When the gas is sampled through the nozzle, it cools in two regions: in the thermal boundary layer surrounding the orifice and in the near-adiabatic expansion downstream of the nozzle throat. This can cause a shift of fast equilibrium reactions in the exothermic direction during sampling. In particular, ion hydrates can be enhanced with respect to the parent ion. These sampling problems have been discussed in

© 1998 NRC Canada

Table 2. Calculated parameters of the $SnOH^+$ ion (2).

Parameter	Calculation A (B3LYP/DZVP)	Calculation B (B3LYP/Sadlej)
Sn—O bond length (Å)	1.931	1.885
O—H bond length (Å)	0.973	0.969
Bond angle (degrees)	154.1	167.9
Rotational temperatures (K)	150.590 11	669.578 11
	0.409 83	0.426 47
	0.408 72	0.426 20
Vibrational temperatures (K)	339.01	120.53
	989.66	1039.94
	5427.05	5521.94

considerable detail (13–15). In general, if the relaxation time τ of an equilibrium reaction is greater than the sampling time of roughly 1 μs, it may be assumed that the reaction does not shift during sampling. In the present study, the problem arising from hydrates of the tin ions, such as $SnOH^+{\cdot}H_2O$ and $Sn^+{\cdot}H_2O$ which are probably not genuine flame ions, is obviated by measuring TPI_{100} such that hydrate contributions are included with the $SnOH^+$ and Sn^+ parent ion signals. At the other extreme, consider for example flame 3 in Table 1 with a rise velocity in the burnt gas of 15.6 m s^{-1}. Appreciable air entrainment is minimal for approximately the first 2.5 flame diameters downstream of the reaction zone; i.e., 30 mm, equivalent to a time of 1.9 ms. For a reaction to reach equilibrium within the time-scale of the flame, clearly τ must be small compared with 1.9 ms.

3. Statistical thermodynamic calculations

For some of the reactions involving tin, some of their properties could not be measured experimentally. Tables of thermodynamic data for many of the ancilliary species involved are listed in the JANAF tables over a wide temperature range (5); for SnO, the free-energy function $-(G_T^\circ - H_{298}^\circ)/T$ and enthalpy function $(H_T^\circ - H_{298}^\circ)$ are tabulated by Pedley and Marshall (3) up to 4000 K. Such data are not available for Sn, Sn^+, and $SnOH^+$, and it was necessary to calculate third-law absolute entropies S_T°, free energy, and enthalpy functions for some of these species by standard statistical methods. A good summary of the relevant formulae is given in the introduction to the JANAF tables (5). For the Sn neutral atom, Moore (4) lists three low-lying electronic states below 10 000 cm^{-1} with corresponding electronic temperatures θ_e (and degeneracies, g values) of 2002.5 K ($g_1 = 3$), 4931.7 K ($g_2 = 5$), and 12 392.3 K ($g_3 = 5$); for the ground state, $g_0 = 1$. For Sn^+ (4), $g_0 = 2$, and there is one low-lying state with $\theta_e = 6116.9$ K ($g_1 = 4$).

The calculation of thermodynamic functions for $SnOH^+$ was made possible by the ab initio calculations of Rodriquez et al. (2). Two of the calculations designated here as A (B3LYP/DZVP) and B (B3YP/Sadlej) each provided a set of rotational and vibrational temperatures, and also structural parameters given in Table 2. Both calculations depict $SnOH^+$ as a bent asymmetric-top molecule with one low vibrational temperature and two very low, nearly equal, rotational temperatures; conceivably, an even higher level calculation might indicate that $SnOH^+$ is linear.[2] The ground electronic state is nondegenerate, and there is no evidence of a low-lying excited state. For calculations A and B, the sum of the rotational and vibrational contributions to the thermodynamic functions had very similar magnitudes. Since there was no reason to prefer one calculation over the other, the results of the two calculations were simply averaged. Largely for reasons of conformity with the JANAF tables (5), a standard state for pressure of 0.1 MPa rather than 1 atm, designated by ° on thermodynamic quantities, was employed for the statistical calculations. Any differences, which only arise for functions involving the entropy, are small and well within the error limits.

4. Composition of neutral tin species in flames

Available spectroscopic evidence indicates that tin is present in flames only as Sn and SnO; the total concentration of tin ions is negligible in comparison. The percentage of each neutral species was found by calculating the equilibrium constant K_1 for the reaction

$$[1] \qquad Sn + H_2O = SnO + H_2$$

The free energy function $-(G_T^\circ - H_{298}^\circ)/T$ over a wide temperature range is available for H_2O and H_2 from the JANAF tables (5) and for SnO from the tables of Pedley and Marshall (3). At any temperature T, K_1 is obtained from $\Delta G_T^\circ[1] = -RT \ln K_1$ with $\Delta G_T^\circ = \Delta H_{298}^\circ - T\Delta\{-(G_T^\circ - H_{298}^\circ)/T\}$ for reaction [1]; $\Delta H_{298}^\circ[1] = -D_{298}^\circ(SnO) + D_{298}^\circ(OH) + D_{298}^\circ(H\text{-}OH) - D_{298}^\circ(H_2) = -42.2$ kJ mol^{-1} (16) based on $D_0^\circ(SnO) = 528 \pm 13$ kJ mol^{-1} (3). A plot of ln K_1 versus $1/T$ gives a very good straight line over the whole temperature range 298.15–2500 K, yielding $K_1 = 1.665 \exp(5140/T)$ from a least-squares fit; specifically over the temperature range 1820–2400 K of the five flames, $K_1 = 1.015 \exp(6064/T)$. The percentage SnO/Sn ratio for the five flames is given in Table 1; in all cases, SnO > 96.9% of the total tin present and SnOH is negligible.

5. Results and discussion

The tin atom has 10 stable isotopes (16) with mass numbers u and natural abundances (%) of 112 (0.97), 114 (0.65), 115 (0.36), 116 (14.53), 117 (7.68), 118 (24.22), 119 (8.58),120 (32.59), 122 (4.63), and 124 (5.79). With the atomizer spraying a 0.1 M aqueous solution of $SnCl_4{\cdot}5H_2O$ into flame 3, a mass spectrum measured at high resolution showing all of the tin ions present downstream at $z = 30$ mm is given in Fig. 1. With increasing mass number, these include H_3O^+, Na^+, a hydrate contribution from $H_5O_2^+$, $^{39}K^+$, $^{41}K^+$, and three groups of isotopic tin peaks above 100 u involving Sn^+, $SnOH^+$ (including a small contribution from $Sn^+{\cdot}H_2O$), and $SnOH^+{\cdot}H_2O$; sodium and potassium are present in the tin salt as impurities.

It is probably helpful to list all of the ionic reactions relevant to this paper in one place. These include

$$[2] \qquad H + H + OH \Leftrightarrow H_3O^+ + e^-$$

---

[2] A.C. Hopkinson. Personal communication.

© 1998 NRC Canada

Fig. 1. Mass spectrum at high resolution measured at z = 30 mm downstream in flame 3 with the atomizer spraying a 0.1 M solution of $SnCl_4 \cdot 5H_2O$.

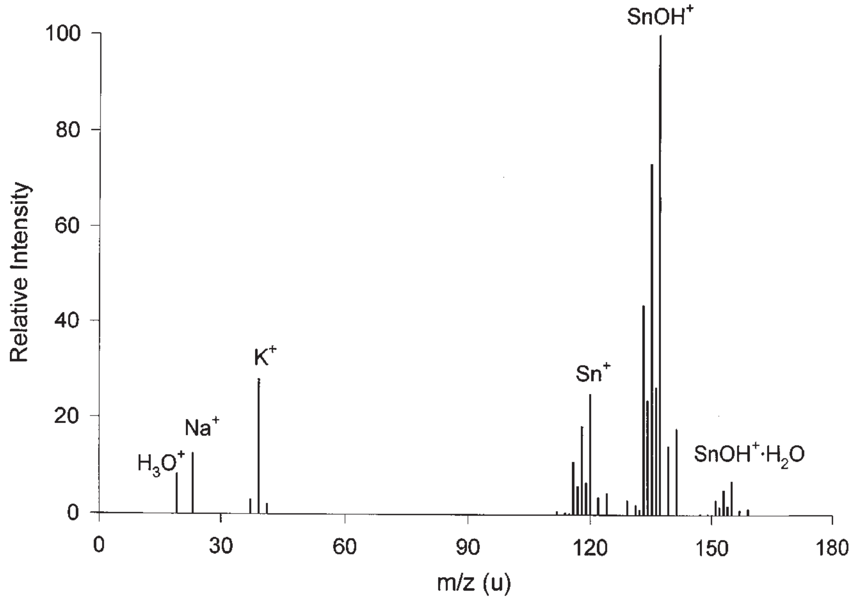

Fig. 2. Ion profiles measured at low resolution in flame 3 with the atomizer spraying a 0.1 M solution of $SnCl_4 \cdot 5H_2O$, where TPI_{12} denotes total positive ions, and TPI_{100} is total ions of tin. The flame reaction zone is located near z = 0.

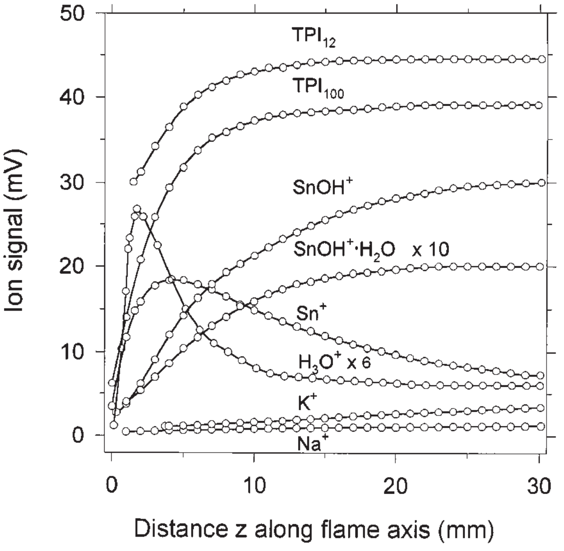

[3] $H_3O^+ + SnO = SnOH^+ + H_2O$

[4] $SnO + H \Leftrightarrow SnOH^+ + e^-$

[5] $SnOH^+ + H = Sn^+ + H_2O$

[6] $Sn^+ + e^- + M \rightarrow Sn + M$

[7] $K + M \rightarrow K^+ + e^- + M$

[8] $Na + M \rightarrow Na^+ + e^- + M$

[9] $H_3O^+ + K \Leftrightarrow K^+ + H_2O + H$

[10] $H_3O^+ + Na \Leftrightarrow Na^+ + H_2O + H$

where M is a third body. Here, the = sign refers to a fast balanced reaction at equilibrium whereas ⇔ refers to a reaction proceeding in both directions which is not necessarily balanced. From this list, it is clear how the ions observed in the mass spectrum arise. The ion hydrates are not included, since they are assumed to form during sampling and are not genuine flame ions.

5.1 The $SnOH^+/H_3O^+$ equilibrium

In H_2-O_2-N_2 flames, the degree of natural ionization is measureable but small, produced by the chemi-ionization reaction [2] with a rate coefficient $k_2 = (3.3 \pm 1.6) \times 10^{-36} \exp(-13\,800/T)$ cm^6 molecule^{-2} s^{-1} (17) and a reverse recombination coefficient already given as $k_{-2} = (3.6 \pm 0.5)T^{-2.1\pm0.7}$ cm^3 molecule^{-1} s^{-1} (10). With the atomizer spraying distilled water (or turned off — the same signal is measured) in each of the five flames, an H_3O^+ profile is obtained (not shown; see (6)) which rises rapidly near the flame reaction zone to a constant plateau value that persists downstream; the magnitude increases with increasing flame temperature. The rapid rise reflects the γ^3-dependence of the three radical concentrations in reaction [2]. When tin is added to a flame, $SnOH^+$ is produced from H_3O^+ by the chemical ionization (CI) reaction [3] involving fast proton transfer, supplemented by the chemi-ionization reaction [4]. Atomic Sn^+ ions are also formed immediately by the fast balanced reaction [5].

Figure 2 presents profiles for the individual ions in flame 3 measured at low resolution with the atomizer spraying a 0.1 M solution of $SnCl_4 \cdot 5H_2O$. For a given tin ion, low resolution effectively blended all the tin isotopes into a single peak and yielded higher sensitivity. The total positive ions TPI_{12} and the total tin ions TPI_{100} are also shown; the difference of these two profiles is the sum of the H_3O^+, Na^+, $H_5O_2^+$, and K^+ profiles. The important point at issue is that, downstream near z = 30 mm, the $SnOH^+$ (+ hydrate) and H_3O^+ profiles are constant, indicative of equilibrium for the fast proton transfer reaction [3] between SnO and H_2O. Even

© 1998 NRC Canada

Fig. 3. Ion profiles measured at high resolution in flame 2 with the atomizer spraying a 0.01 M solution of $SnCl_4 \cdot 5H_2O$. The flame reaction zone is located near $z = 0$.

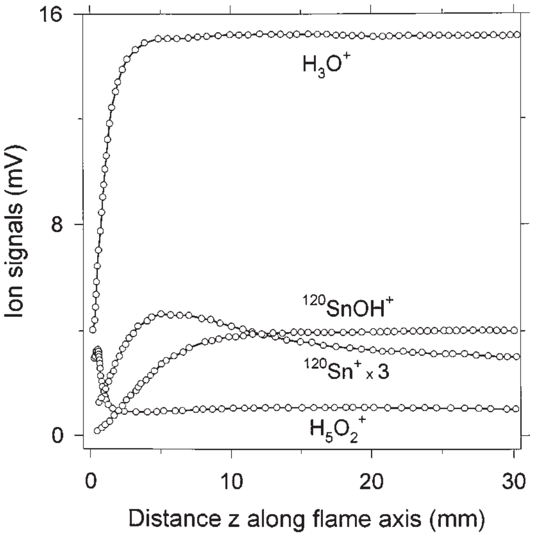

though the reaction is strongly exoergic, the large concentration ratio $[H_2O]/[SnO] \approx 3 \times 10^5$ can still bring the H_3O^+ and $SnOH^+$ ions into equilibrium in flames. Furthermore, the relaxation time $\tau_3 = 1/(k_3[SnO] + k_{-3}[H_2O])$ is of the order of 100 μs, appreciably greater than the sampling time of roughly 1 μs, such that the equilibrium reaction [3] does not shift during sampling. For this estimate, a typical value of k_3 for a proton transfer reaction of the order of 10^{-9} cm^3 molecule^{-1} s^{-1} was assumed (k_3 would be somewhat higher at flame temperature than room temperature). A value for k_{-3} for the reverse reaction was estimated to be that for k_3 reduced by an exponential factor corresponding to the approximate endothermicity of the back reaction.

The objective of this aspect of the study was to measure the ion ratio $[SnOH^+]/[H_3O^+]$ to get the equilibrium constant K_3 giving $\Delta H^\circ[3]$ from the slope of a van't Hoff plot of ln K_3 versus $1/T$ where $\Delta H^\circ[3] = PA^\circ(H_2O) - PA^\circ(SnO)$, the difference of the proton affinities. There is another important feature of this method involving the measurement of K_3 in five flames spanning nearly 600 K. Suppose the two ion signals are subject to mass discrimination leading to an incorrect value of $K_3' = f \times K_3$ where f is a constant factor which is independent of temperature. The slope of the van't Hoff plot will still yield the correct value of $\Delta H^\circ[3]$ although the intercept will be $(\Delta S^\circ[3]/R + \ln f)$. It will be shown in the next section that reaction [5] producing Sn^+ shifts to the right during sampling such that measured values of $[SnOH^+]$ are slightly small by a nearly constant factor f which is only very weakly dependent on temperature. This is similar to the case of mass discrimination, and good values of $\Delta H^\circ[3]$ are still obtained.

By way of contrast, the profiles in Fig. 3 were measured at high resolution in the hot flame 2 with the atomizer spraying a 0.01 M solution of $SnCl_4 \cdot 5H_2O$. Again, the $SnOH^+$ and H_3O^+ profiles are constant downstream, indicative of equilibrium. In this case, only the single biggest isotopic peak $^{120}SnOH^+$ was measured, and $[H_3O^+] > [^{120}SnOH^+]$ at the lower tin concentration. For plotting purposes, the ^{120}Sn isotopic signals were multiplied by 100/32.59 to give 100% Sn signals. Figure 4 presents a van't Hoff plot of ln K_3 versus $1/T$ for the two runs with the 0.1 and 0.01 M solutions sprayed into five flames. From the slope of the straight line fitted by least squares, $\Delta H^\circ_{2100}[3] = -218.0 \pm 10.5$ (standard deviation) kJ mol^{-1} over the flame temperature range 1820–2400 K centred on the average temperature of 2100 K.

Fig. 4. Van't Hoff plot for the equilibrium constant of the proton transfer reaction [3] involving H_3O^+ and $SnOH^+$ measured in five flames over the temperature range 1820–2400 K with the atomizer spraying aqueous solutions of $SnCl_4 \cdot 5H_2O$ of concentrations 0.1 M (open circles) and 0.01 M (closed circles).

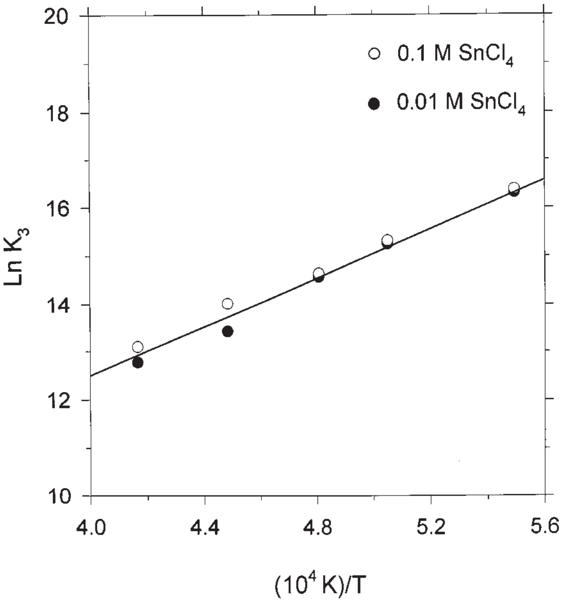

To obtain $PA^\circ_{298}(SnO) = PA^\circ_{298}(H_2O) - \Delta H^\circ_{298}[3]$, the reaction enthalpy at 298.15 K is required, derived from $\Delta H^\circ_{298} = \Delta H^\circ_{2100} - \Delta(H^\circ_{2100} - H^\circ_{298})$ where the standard enthalpy function $(H^\circ_{2100} - H^\circ_{298})$ is available for H_3O^+, H_2O (5), and SnO (3) but not for $SnOH^+$. Accordingly, it was calculated by statistical methods at the average flame temperature of 2100 K. For reaction [3], the temperature correction is small; $\Delta(H^\circ_{2100} - H^\circ_{298}) = 1.82$ kJ mol^{-1} giving $\Delta H^\circ_{298}[3] = -219.8 \pm 10.5$ kJ mol^{-1}. Based on the current value of $PA^\circ_{298}(H_2O) = 691.0$ kJ mol^{-1},[3] the proton affinity of SnO has a value $PA^\circ_{298}(SnO) = 911 \pm 21$ kJ mol^{-1} = 218 ± 5 kcal mol^{-1}, in excellent agreement with the calculated value of 215.6 kcal mol^{-1} obtained by Rodriquez et al. (2).

5.2 The $SnOH^+/Sn^+$ equilibrium

The equilibration of $SnOH^+$ and Sn^+ by reaction [5] is rapid in flames. If $k_5 = 10^{-9}$ cm^3 molecule^{-1} s^{-1} is assumed with k_{-5} reduced by a factor corresponding to the endothermicity of the back reaction (approximately 100 kJ mol^{-1}), the relaxation time $\tau_5 \approx 0.1$ μs. This means that the reaction will shift to the right in the exothermic direction during sampling, and measured $[SnOH^+]/[Sn^+]$ ratios will be too small.

---

[3] E.P. Hunter and S.G. Lias. NIST Standard Database Number 69. March 1998 release. http://webbook.nist.gov/chemistry/form-ser.html/

© 1998 NRC Canada

Fig. 5. Ion profiles measured in flame 3 with 0.25 mol% of added CH_4 and the atomizer spraying a mixed solution of 0.098 M $SnCl_4 \cdot 5H_2O$ and 0.001 M KNO_3 such that electron–ion recombination of $SnOH^+$ is the dominant process downstream; TPI_{12} denotes total positive ions and TPI_{100} is total ions of tin. The flame reaction zone is located near z = 0.

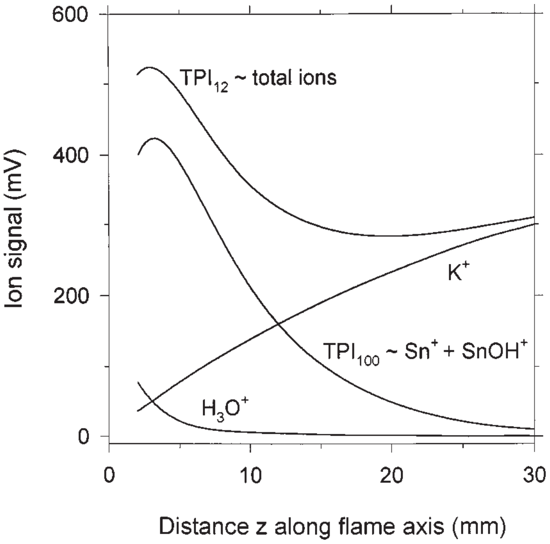

Since absolute $SnOH^+$ concentrations were needed for the recombination studies described below, it was necessary to calculate the equilibrium constant K_5 as a function of temperature. In this way, total tin ion signals $[TPI_{100}]$ could be measured and true $[SnOH^+]$ determined using K_5.

The free energy function $-(G^\circ_T - H^\circ_{298})/T$ was calculated by statistical methods for $SnOH^+$ and Sn^+ at many temperatures up to 2500 K and combined with corresponding values from the JANAF tables (5) for H and H_2O to obtain $\Delta G^\circ_T - \Delta H^\circ_{298}$ for reaction [5]. Using all values at 298.15 K (16) and our value of $PA^\circ_{298}(SnO)$ = 910.8 kJ mol^{-1}, $\Delta H^\circ_{298}[5] = PA^\circ(SnO) - IE^\circ(H) + D^\circ(SnO) + IE^\circ(Sn) - D^\circ(OH) - D^\circ(H\text{-}OH) = -86.3$ kJ mol^{-1}, giving ΔG°_T and thus K_5. A plot of ln K_5 versus $1/T$ gives a very good straight line over the range of flame temperatures 1820–2400 K with a least-squares fit represented by K_5 = 0.077 38 exp (11 450/T). In fact, a good straight line is obtained over the whole temperature range of 298–2500 K fitted by K_5 = 0.1115 exp (10 890/T). The entropy change of reaction [5] was calculated to be $\Delta S^\circ_{2100} = -21.2$ and $\Delta S^\circ_{298} = -6.4$ J mol^{-1} K^{-1}. The reaction enthalpy has a value $\Delta H^\circ_{2100} = -94.8$ kJ mol^{-1} at the average flame temperature with $\Delta H^\circ_0 = -84.3 \pm 20.9$ kJ mol^{-1} (= ΔE°_0), in reasonable agreement with the value arrived at by Jensen (1). He quotes a value $\Delta E^\circ_0[5] = -100 \pm 20$ kJ mol^{-1} based on mass-spectrometric measurements of the $[SnOH^+]/[Sn^+]$ ratio at two flame temperatures and a rough statistical calculation with vibrational temperatures estimated from those of the alkaline earth metals. His ion ratio measurements may not have been shifted appreciably by sampling cooling because, to the best of our knowledge, he was employing low-pressure flames (P = 1–10 Torr) in his mass spectrometer (18); since the relaxation time $\tau \propto 1/P$, its magnitude in his experiment may have exceeded the sampling time of approximately 1 μs.

5.3 Recombination of $SnOH^+$ with electrons

These hydrogen flames contain a small amount of H_3O^+ natural ionization formed by the chemi-ionization reaction [2], and $SnOH^+$ is formed by chemical ionization (CI) of SnO by H_3O^+ via the proton transfer reaction [3]. A further possible source of $SnOH^+$ is the chemi-ionization reaction [4]. To study the recombination reaction [–4], the objectives were to form a relatively high concentration of $SnOH^+$ rapidly near the flame reaction zone and then to assure that recombination was dominant downstream in the burnt gas. These conditions were achieved, first by adding 0.25 mol% of CH_4 to produce a superequilibrium level of H_3O^+ for CI by reaction [3]. Then, a small amount of potassium as KNO_3 was added to the atomizer solution to raise the concentration of free electrons in the flame, thereby enhancing the rate of recombination of $SnOH^+$ by reaction [–4]. Potassium atoms are chemically ionized initially by H_3O^+ to some extent by reaction [9] (19) but progressively ionize further downstream by collisional (thermal) ionization via reaction [7] (20). There is no evidence that potassium interacts with tin by any process other than its effect on recombination through $[e^-]$. It was necessary to adjust the relative concentrations of both $SnCl_4 \cdot 5H_2O$ and KNO_3 in the atomizer solution rather carefully so that (*i*) H_3O^+ disappears quite rapidly downstream to maximize the region in which $SnOH^+$ recombination is dominant, and (*ii*) $[SnOH^+]$ falls to a value near zero at z = 30 mm downstream indicating that $SnOH^+$ ion production by the chemi-ionization reaction [4] was negligible.

Figure 5 presents profiles for flame 3 with added CH_4 and with the atomizer spraying a mixed aqueous solution of 0.098 M $SnCl_4 \cdot 5H_2O$ and 0.001 M KNO_3. At these concentrations, the profiles fulfil the conditions outlined in (*i*) and (*ii*) above. The TPI_{100} signal includes $SnOH^+$, Sn^+, and any hydrates formed during sampling. Since negative ions were not detected in these flames, the TPI_{12} profile which measures the sum of all positive ions gives $[e^-]$ because a flame is a quasi-neutral plasma. From reaction [–4], $-d[SnOH^+]/dt = k_{-4}[SnOH^+][e^-]$ – (ion production term) with $v = dz/dt$ = 15.6 m s^{-1} from Table 1. Differentiation of $[TPI_{100}]$ gives the kinetic expression $-d[TPI_{100}]/dt = -d[SnOH^+]/dt - d[Sn^+]/dt = k_{-4}[SnOH^+][e^-] + k_6[Sn^+][e^-] - k_4[SnO][H]_{eq}\gamma$ in which the equilibrated reaction [5] does not appear. The assumptions are made that three-body recombination of atomic Sn^+ in reaction [6] is negligible compared with reaction [–4], and that the production term from reaction [4] can be ignored because of the experimental conditions set up; also, reaction [3] does not contribute downstream where $[H_3O^+] \approx 0$. Since $[SnOH^+] = [TPI_{100}]/(1 + K_5[H]_{eq}\gamma/[H_2O])$, the kinetic expression reduces to $-v(d[TPI_{100}]/dz)(1 + K_5[H]_{eq}\gamma/[H_2O]) = k_{-4}[TPI_{100}][TPI_{12}]$. Note that the factor $(1 + K_5[H]_{eq}\gamma/[H_2O])$, which has been multiplied across to the left-hand side, is equivalent to $(1 + [Sn^+]/[SnOH^+])$; the ion ratio is small compared with unity, varying from 0.13 in flame 2 to 0.06 in flame 5.

For the final kinetic expression, Fig. 6 presents a plot for flame 3 of the left-hand side versus $[TPI_{100}][TPI_{12}]$ in the range z = 15–30 mm where $[H_3O^+] \approx 0$. The slope of the plot gives the recombination coefficient $k_{-4} = 3.6 \times 10^{-7}$ cm^3 molecule^{-1} s^{-1} in this particular case. The small negative in-

© 1998 NRC Canada

Fig. 6. Plot involving the kinetic expression for $SnOH^+$ ion loss by electron–ion recombination by reaction [–4] for the range z = 15–30 mm downstream in flame 3 using the ion profiles presented in Fig. 5, where the slope yields the recombination coefficient k_{-4}.

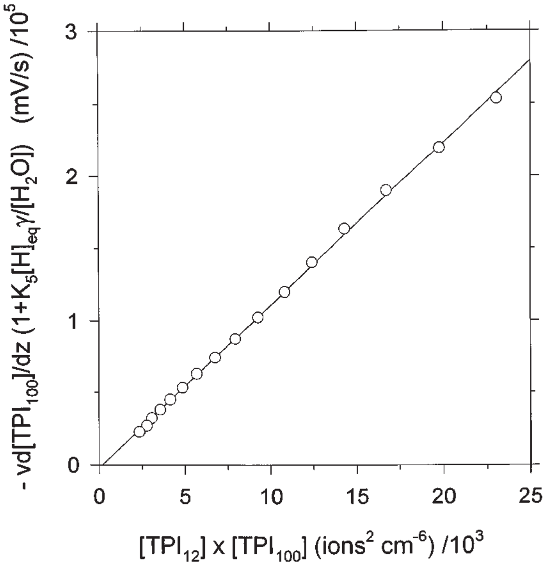

Fig. 7. Logarithmic plot of the recombination coefficient k_{-4} versus temperature T in the range 1820–2400 K. The best-fit solid line exhibits a $T^{-1.7}$ dependence, for comparison with the broken line giving the $T^{-1.5}$ dependence expected from simple theory.

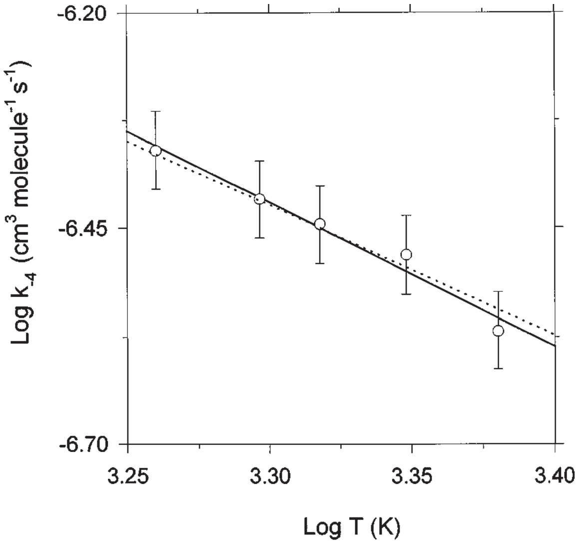

tercept shows that ion production is small and can safely be ignored. Similar profiles were measured and plots made to evaluate k_{-4} in all five flames. The results over the temperature range 1820–2400 K are given in Fig. 7 as a plot of log k_{-4} versus log T. A straight line fitted by least squares gives the temperature variation as $k_{-4} = (0.116 \pm 0.065)T^{-(1.66 \pm 0.16)}$ cm^3 molecule^{-1} s^{-1}. A discussion of the temperature dependence of electron-ion recombination coefficients in flames has been given by Butler and Hayhurst (10). Simple theory indicates a $T^{-1.5}$ dependence with which our value is in good agreement.

5.4 Chemi-ionization of SnO + H

Repeated attempts were made to measure the rate constant of the chemi-ionization reaction [4] directly but were frustrated by the presence of tiny amounts of potassium and sodium in the salt sample of $SnCl_4 \cdot 5H_2O$. These impurities give rise to the K^+ and Na^+ peaks visible in the mass spectrum shown in Fig. 1 which arise initially upstream by the electron transfer reactions [9] and [10] (19), and further downstream by the collisional (thermal) ionization reactions [7] and [8] (20). The initial rise of the $SnOH^+$ profile in Fig. 2 stems from proton transfer by reaction [3]. This means that the growth of the $SnOH^+$ profile in the upstream region cannot be analysed for k_4. Figure 2 also shows how the K^+ and Na^+ signals grow downstream by thermal ionization to increase [e$^-$]. Furthermore, k_4 cannot be readily evaluated from the constant $SnOH^+$ profile downstream near z = 30 mm because reaction [4] is not at equilibrium. The relaxation time is given by $\tau_4 = \{\ln(2e - 1)\}/2(k_4 k_{-4}[SnO][[H])^{1/2}$ which has a value of the order of 10 ms for a 0.1 M solution of $SnCl_4 \cdot 5H_2O$ sprayed by the atomizer and $k_4 \approx 10^{-20}$ cm^3 molecule^{-1} s^{-1} at 2100 K (derived below); equilibrium cannot be achieved in the time of approximately 2 ms corresponding to 30 mm of flame. The same conclusion was reached by Jensen (1). A final consideration is that the rate of collisional (thermal) ionization $R_7 \approx 10^8$ ions cm^{-3} s^{-1} even for a tiny (unknown) potassium impurity concentration of 10^{-7} M in the atomizer solution (20); the rate R_4 for the chemi-ionization of tin is very comparable, and certainly not dominant. Although the experiments were not successful, these considerations seemed worthy of discussion because they indicate the complete ionization picture and may apply to other metals with small rate coefficients for chemi-ionization.

Accordingly, the equilibrium constant K_4 for reaction [4] was obtained by statistical methods, again involving the free energy function $-(G^\circ_T - H^\circ_{298})/T$ calculated for $SnOH^+$ and available for SnO (3), H and e$^-$ (5). At any temperature T, this gives $\Delta\{-(G^\circ_T - H^\circ_{298})/T\} = R \ln K_4 + \Delta H^\circ_{298}/T$ with $\Delta H^\circ_{298}[4] = -\mathrm{PA}^\circ_{298}(\mathrm{SnO}) + \mathrm{IE}^\circ_{298}(\mathrm{H}) = 407.4$ kJ mol^{-1}. Over the temperature range 1820–2400 K of the five flames, a plot of ln K_4 versus $1/T$ gave a very good straight line from which $K_4 = 0.004\,868 \exp(-52\,070/T)$. Over the whole temperature range 298.15–2500 K, a similar plot gave a good straight line yielding $K_4 = 0.001\,324 \exp(-49\,710/T)$.

For reaction [4], other channels in both the forward and reverse directions are unlikely, and the assumption of detailed balance is reasonable. Using K_4 in the range of flame temperatures, the rate constant for chemi-ionization is obtained from $k_4 = k_{-4}K_4$. When combined with the experimental values of k_{-4} in the five flames, values of k_4 are obtained ranging from 5.03×10^{-19} in flame 2 at 2400 K to 8.07×10^{-22} cm^3 molecule^{-1} s^{-1} in flame 5 at 1820 K. A plot of ln k_4 versus $1/T$ is shown in Fig. 8. A good straight line fitted by least squares through the data points gives $k_4 = 3.27 \times 10^{-10} \exp(-48\,630/T)$ cm^3 molecule^{-1} s^{-1} for the temperature range 1820–2400 K. Even at flame temperatures, the values of the rate constant are small but should have been measureable experimentally were it not for the presence of potassium and sodium as impurities.

Fig. 8. Semi-logarithmic plot giving the temperature variation of the rate constant as ln k_4 versus $1/T$ for the chemi-ionization reaction [4] in the range 1820–2400 K.

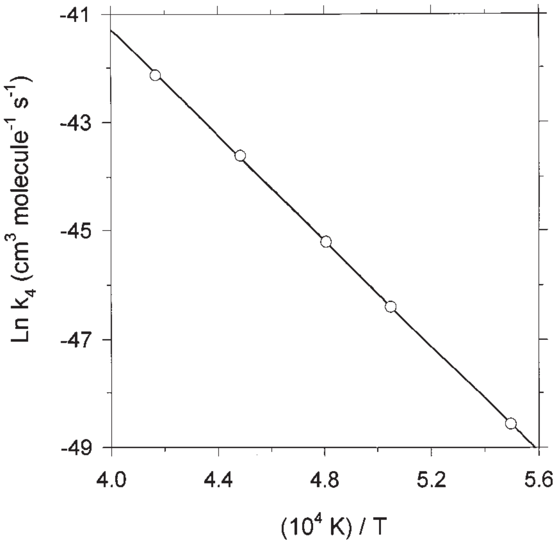

5.5 Bond energy D_0°(HO-Sn$^+$) and $\Delta_f H_0^\circ$(SnOH$^+$)

The standard Sn—O bond dissociation energy for the SnOH$^+$ ion can be found from the calculated change in the enthalpy function for the dissociation reaction

$$[11] \quad SnOH^+ \rightarrow Sn^+ + OH$$

with reference to reaction [5]; i.e., $\Delta\{H_{298}^\circ - H_0^\circ\}[11] = 3.49$ kJ mol^{-1} = $\Delta H_{298}^\circ[11] - \Delta H_0^\circ[11] = \Delta H_{298}^\circ[5] + D_{298}^\circ$(H—OH) – D_0°(HO—Sn$^+$). This gives a value for the bond energy D_0°(HO—Sn$^+$) = 408 ± 21 kJ mol^{-1} (98 ± 5 kcal mol^{-1}). Finally, the standard zero-point enthalpy of formation $\Delta_f H_0^\circ$(SnOH$^+$) can be obtained from $\Delta H_0^\circ[5] = -84.3$ kJ mol^{-1} with $\Delta_f H_0^\circ$(Sn$^+$) = 1010.6 (21), $\Delta_f H_0^\circ$(H$_2$O) = –238.9 and $\Delta_f H_0^\circ$(H) = 216.0 kJ mol^{-1} (5). The value is $\Delta_f H_0^\circ$(SnOH$^+$) = 640 ± 21 kJ mol^{-1} (153 ± 5 kcal mol^{-1}); at room temperature, $\Delta_f H_{298}^\circ$(SnOH$^+$) = 637 ± 21 kJ mol^{-1}. It is in good agreement with Jensen's value stated as the equivalent function $\Delta_f E_0^\circ$(SnOH$^+$) = 655 ± 27 kJ mol^{-1} estimated nearly 30 years ago from a crude statistical model.

6. Summary and conclusions

The ionization of tin was investigated in H_2-O_2-N_2 flames in the range 1820–2400 K by mass-spectrometric sampling. The study was greatly aided by data for rotational and vibrational temperatures of the SnOH$^+$ ion from ab initio calculations (2) so that thermodynamic functions could be calculated by statistical mechanics. If total tin is present only as SnO and Sn, SnO > 97% in these fuel-rich flames. The flame conditions are such that SnOH$^+$ can be measured in equilibrium with H_3O^+, leading to the proton affinity PA°(SnO) relative to that of H_2O. The rapid equilibration of SnOH$^+$ with Sn$^+$ cannot be measured because it is shifted to a lower unknown temperature during sampling, but its equilibrium constant could be determined by a statistical thermodynamic calculation. This provided correct values of the SnOH$^+$ concentration for the experimental measurement of the electron-ion recombination coefficient of SnOH$^+$ as a function of temperature. Its $T^{-1.7}$ temperature dependence is close to the $T^{-1.5}$ dependence predicted by simple theory. The recombination reaction is the backward direction of the chemi-ionization reaction of SnO + H. Its relatively small rate coefficient could not be measured experimentally due to the ionization of potassium and sodium present as impurities in the tin salt. However, the equilibrium constant for chemi-ionization/recombination could be calculated by statistical methods. Assuming detailed balance, the rate coefficient for chemi-ionization as a function of temperature was obtained as the product of the experimental recombination coefficient and calculated equilibrium constant. Finally, the bond strength D_0°(HO—Sn$^+$) could be calculated, and also the standard zero-point enthalpy of formation $\Delta_f H_0^\circ$(SnOH$^+$). This study combines experiment with theoretical calculations to give a fairly complete analysis of tin ionization.

Acknowledgement

The authors wish to thank Prof. Alan C. Hopkinson and members of his group for helpful discussions, and for making available to us the details of their ab initio calculations of the SnOH$^+$ ion. Support of this work by the Natural Sciences and Engineering Research Council of Canada is gratefully acknowledged.

References

1. D.E. Jensen. J. Chem. Phys. **51**, 4674 (1969).
2. C.F. Rodriquez, A. Cunje, and A.C. Hopkinson. J. Mol. Struct. (Theochem), **430**, 149 (1998).
3. J.B. Pedley and E.M. Marshall. J. Phys. Chem. Ref. Data, **12**, 967 (1983).
4. C.E. Moore. Natl. Stand. Ref. Data Ser. Natl. Bur. Stand. (U.S.) (NSRDS–NBS) 35. Vol. 3. Superintendent of Documents, U.S. Government Printing Office, Washington, D.C. Reissued 1971 (from NBS Circ. 467, 1958).
5. M.W. Chase, Jr., C.A. Davies, J.R. Downey, Jr., D.J. Frurip, R.A. McDonald, and A.N. Syverud. JANAF thermochemical tables. 3rd ed. J. Phys. Chem. Ref. Data, **14** (Suppl. 1) (1985).
6. C.J. Butler and A.N. Hayhurst. J. Chem. Soc. Faraday Trans. **93**, 1497 (1997).
7. A.N. Hayhurst and D.B. Kittelson. Proc. R. Soc. London A, **338**, 155 (1974).
8. J.M. Goodings, C.S. Hassanali, P.M. Patterson, and C. Chow. Int. J. Mass Spectrom. Ion Processes, **132**, 83 (1994).
9. J.M. Goodings, S.M. Graham, and W.J. Megaw. J. Aerosol Sci. **14**, 679 (1983).
10. C.J. Butler and A.N. Hayhurst. J. Chem. Soc. Faraday Trans. **92**, 707 (1996).
11. J.M. Goodings and P.M. Patterson. Int. J. Mass Spectrom. Ion Processes, **151**, 17 (1995).
12. S.D.T. Axford and A.N. Hayhurst. Int. J. Mass Spectrom. Ion Processes, **110**, 31 (1991).
13. A.N. Hayhurst, D.B. Kittelson, and N.R. Telford. Combust. Flame, **28**, 123 (1977).
14. A.N. Hayhurst and D.B. Kittelson. Combust. Flame, **28**, 137 (1977).
15. N.A. Burdett and A.N. Hayhurst. Combust. Flame, **34**, 119 (1979).
16. D.R. Lide (*Editor*). CRC handbook of chemistry and physics. 73rd ed. CRC Press, Boca Raton, Fla. 1992.
17. S.D.T. Axford and A.N. Hayhurst. J. Chem. Soc. Faraday Trans. **91**, 827 (1995).

© 1998 NRC Canada

18. H.F. Calcote. *In* Ion-molecule reactions. Vol. 2. *Edited by* J.L. Franklin. Plenum Press, New York. 1972. p. 673.
19. A.N. Hayhurst and N.R. Telford. Trans. Faraday Soc. **66**, 2784 (1970).
20. A.F. Ashton and A.N. Hayhurst. Combust. Flame, **21**, 69 (1973).
21. S.G. Lias, J.E. Bartmess, J.F. Liebman, J.L. Holmes, R.D. Levin, and W.G. Mallard. J. Phys. Chem. Ref. Data, **17** (Suppl. 1) (1988).

© 1998 NRC Canada